ERJ
Engineering Research Journal
Faculty of Engineering
Minoufiya University

USE OF GEOTEXTILE AS A REINFORCEMENT FOR FLEXIBLE PAVEMENT OVERLAY

S.A. El-Hamrawy*, H.A. Afify, U.G.Abdel-Mageed****

**Faculty of Eng., Minoufiya University **Faculty of Eng., Tanta University.*

Abstract

Pavement distresses are numerous and they differ in their shape, type, and origin causes. Cracking is one of the most commonly observed distresses in asphalt pavement. Hence if these cracks reflect up to the new overlay, this reduce the service life and the serviceability of the pavement thus lead to a heavy burden on the exchequer. This investigation studies the effect of reinforcing the new overlay by geotextile and its influence on the performance of pavement and on retarding the speed of reflective cracking propagation. So asphaltic beam specimens reinforced with two types of reinforcement (**ALYAF PU 14** nonwoven geotextile and **HaTelit c** reinforced geogrid) in the middle as well as in the lower third of the beam depth were tested under the three – point bending test. The prepared beams include beams with and without initial crack to simulate the cracked and uncracked layers in the field. The results of three – point bending test were collected and analyzed by fracture mechanics parameters (fracture toughness KIC, GIC, and J–Integral) and crack depth ratio, Zr, at failure.

Results show that involving the reinforcement can relevant the speed of crack propagation into the new overlay and consequently prolong the economic life of the construction. Improve load - carrying capacity via reducing the tensile stress peaks, absorbing some horizontal tensile stresses, and providing a uniform distribution of loads over a large area. Also **HaTelit c** geogrid appeared results better than **Alyaf PU 14** nonwoven geotextile.

تعتبر الشروخ من أشهر أنواع العيوب فى الرصف الأسفلتى. وإذا ما انعكست الشروخ إلى طبقة الرصف الجديدة فإن ذلك يقلل من عمر الرصف ويقلل من قدرته على الأداء الجيد.

لذلك فإن هذا البحث يدرس تأثير تسليح طبقات الرصف باستخدام الجيوتكستيل وتأثير ذلك على أداء الرصف وعلى إعاقة سرعة انتشار الشروخ الإنعكاسية. ولقد تم تحضير كمرات من الخرسانة الأسفلتية المدموكة ومسلحة بنوعين من الجيوتكستيل (**ALYAF PU 14** and **HaTelit c** geogrid) فى منتصف الكمرة وأعلى الثلث السفلى وتم اختبار تلك الكمرات تحت اختبار عزم الإنحناء ذو الثلاث نقاط. وتم تجهيز نوعين من الكمرات ، الأول ذو شروخ سابقة التجهيز والثانى بدون شروخ لكى تتم محاكاة الطبقات المشرخة والغير مشرخة فى الطبيعة. وتم تحليل النتائج باستخدام طريقتين الأولى طريقة معاملات ميكانيكا الكسر (fracture toughness KIC, GIC, and J–Integral) والثانية طريقة نسبة عمق الشرخ عند الانهيار (Zr).

ولقد أوضحت النتائج أن استخدام التسليح يعوق سرعة نمو الشروخ فى الطبقات العلوية وبالتالى يؤدى إلى زيادة عمر الرصف. والتسليح يؤدى إلى توزيع منتظم للحمل على مساحة أكبر. وأظهرت النتائج أيضاً أن النوع **HaTelit c** geogrid يعطى نتائج أفضل من النوع الغير منسوج **ALYAF PU 14**.

Keywords: reflective cracking – Geotextile – Flexible Pavement – Fracture Mechanics – Bending Test.

1. INTRODUCTION

1.1. General

Many field and laboratory studies indicated that cracking is a problem as serious as that of stability. Various material characterization approaches have been applied to predict and minimize such cracking. In addition, innovative materials such as polymers, reinforcement, and stone mastic asphalt have been introduced into the asphalt construction industry.

The surface cracking, whether it is load associated or reflective in nature, can cause deterioration of bituminous overlay mainly due to the ingress of water into the pavement body through the cracks. Damage can also occur in the form of pumping of soil particles rather than the progressive degradation of road structure in the neighborhood of the cracks caused by local stress concentration. When the damages exceed a certain level, the service life of asphalt layers decreases thus the maintenance is needed. If we can retard or prevent these cracks from reaching to the top layers, the pavement can serve for a long time hence the periods between the maintenance processes can prolong resulting in a decreasing in burden on the exchequer

1.2. Objective

The main objective of this research is using one of the most successful new technologies, that use a combination of bituminous surfacing materials with geotextile, to improve the behavior of asphalt mixes. More specifically, the objectives of this research are:

- Determination of the reinforcement effect on the strengthening of the asphaltic overlay layer.
- Assessment of the best position of reinforcement placement whether in the middle or in the lower third of the overlay depth.
- Studying the reinforcement effect on the resistance of crack propagation.
- Comparison between **ALYAF PU 14** nonwoven geotextile and **HaTelit c** reinforced geogrid in strengthing asphalt mixes.

2. BACKGROUND

The traffic–associated distresses are related to the intensity, configuration, and repetitions of loading. While the non traffic–associated deals with the climatic conditions, subgrade soil, and pavement material properties. Only reflection and fatigue cracking will be discussed.

2.1. Reflection Cracking

The propagation of an existing cracking pattern from the old pavement into and through a new overlay is known as *reflective cracking*. This phenomena happens when the stresses in the overlay become greater than the shear or tensile strength of the hot mix asphalt [1].

As a result of the service loading, the repeated traffic loading or thermal induced stresses due to the drop of temperature from the day temperature to a cold night, the pavement will shrink. This will results in a widening of existing cracks in the underlying pavement. This widening will induce an additional tensile strain at the interface above the crack front. In addition, the presence of the crack itself will create stress concentration at the crack front as suggested by the theory of fracture mechanics [2].

J.M. Rigo 1993 [3] stated methods that have been used to minimize reflection cracking of asphalt concrete overlays in the form of:

a. greater thickness of overlay,
b. changes in the viscosity of asphalt binder,
c. additives incorporated into the asphalt concrete mixture,
d. treatments to the existing pavement before overlying (seal coats, heater-scarifying, crack filling, pavement breaking, stabilization and recycling),and
e. stress relieving interlayers (asphalt-rubber, membranes, fabrics, low-viscosity asphalt cement, and open graded asphalt concrete).

Harold I. et al, 1979 [4] studied the reflection cracking for asphaltic concrete overlays. They said that the basic mechanisms leading to the development of reflection cracking are horizontal and differential vertical movements between the original pavement and the overlay.

B.J. Dempsey, 2002 [5] studied the effect of Interlayer Stress Absorbing Composite (ISAC) on mitigating the problem of reflection cracking in an AC overlay. Performance of ISAC was evaluated by comparing the cycles to failure of an ISAC treated overlay with a control section without ISAC and with two commercially available products. The laboratory evaluation studies indicated that the ISAC system vastly outperformed the control section and the two commercial products tested. Several years of field performance testing have shown that the ISAC system is highly effective for mitigating reflective cracking in AC overlays used on both airport and highway pavement systems.

Ponniah E. Joseph, 1987 [6] conducted a research to study the low temperature reflection cracking through asphalt overlays. He stated that the propagation of cracks through asphalt pavement overlays occurs above the underlying cracks or joints of an existing old pavements is the phenomenon which popularly termed "Reflection Cracking". If an overlay is to be constructed on a cracked or jointed pavement, most of the existing cracks will quickly reflect through the overlay as well. This can decrease the structural strength of the pavement and allows the ingress of water leading to further deterioration of the overlay surface.

2.2. Fatigue cracking

Application of traffic load to the pavement surfaces generates tensile stresses at the bottom of the asphalt layer. Since the tensile strength of asphalt concrete is typically higher than the stress caused by the traffic loading, the material will remain without crack for a number of load applications. With the continuous repetition of load applications, fatigue cracks initiate at weak spots at the bottom of the asphalt layer. These cracks will then propagate through the asphalt layer until they reach the surface [7,8].

Akhtar, 1992 [9] stated that the fatigue resistance of an asphalt mixture is the ability of mix to withstand repeated bending without fracture. In the design of asphalt concrete pavements, it is important to have a measure of the fatigue characteristics of specific mixture over a range of traffic and environmental conditions so that the fatigue conditions can be incorporated in the design process.

Pell, 1967 [10] investigated the effect of mineral filler on the fatigue life. He concluded that at a given stress level, the fatigue life improved as the percentage filler increases beyond a certain level and again decreases when the percentage filler increases more.

Jacobs et al. [11] compared FEM simulation to experimental crack growth of HMA. Although the level of agreement is highly influenced by the mix nominal aggregate size (better agreement was found for mixes with small agg. size), the crack growth process in HMA might be accurately described using the fracture mechanics theory.

3. EXPERIMENTAL WORK

An experimental program was performed to apply the fracture mechanics approach and effective depth method (German method) using three – point bending test applied on the asphalt beams. So the crack propagation in asphalt mixture can be studied under different conditions of reinforcement type, and reinforcement position along the beam depth.

3.1. Materials

3.1.1. Aggregate and asphalt

The coarse and fine aggregate that used in the asphalt mix are crushed dolomite and siliceous sand with 2.60 gm/cm^3 and 2.65 gm/cm^3 bulk density respectively, while limestone dust with bulk density of 2.70 gm/cm3 was used as a mineral filler. Asphalt cement (60/70) penetration grade was used as a binder. The penetration of the asphalt was 67 (1/10 mm) and its softening point was 50 ^oC .

3.1.2. Geotextiles

Two types of geotextiles were used (**Alyaf PU 14** nonwoven geotextile and **HaTelit c** reinforced geogrid) as reinforcement for asphalt concrete mixtures. These types are considered of geotextile products and their technical specifications are shown in Tables 1,2.

- Determination the modulus of elasticity for geotextiles:

Testing of the reinforcement fiber (**HaTelit c** and **Alyaf PU 14**) was performed to determine the modulus of elasticity. For **Alyaf PU 14** specimens, 60 mm. wide with 30 mm. gauge length were tested. An aspect ratio (specimen width / specimen length ratio) of 2 was considered, according to ASTM D 4595, high enough to ensure that "necking" and "roping'' of the geotextile does not occur. The filament (strand) of **HaTelit c** geogrid has a length of 100 mm. with a diameter equal 0.75 mm.

The specimens were mounted on the loading heads of testing machine (jaws). The test was performed at room temperature of 24 °C and loading rate of 0.1 mm./min was used. Modulus of elasticity was 920 and 6640 N/mm2 for **Alyaf PU14** and **HaTelt C** respectively.

Table 1. Technical Specifications of ALYAF PU 14

Properties	Test Method	Spec.
Fabric Weight, g/m2	ASTM D 5261	200
Thickness Under 2 KN/m^2, mm	ASTM D 5199	2.4
Tensile Strength - strip test (5 cm) - Elongation at Max Load, KN/m %	 DIN 53857 DIN 53857	 9.5/11 >70
Asphalt Retention,gal/yd2	Task Force	0.42
Burst Strength	ASTM D 3786	275
Melting Point	-	256 °C

3.2. Specimen Fabrication

The gradation of asphalt – aggregate mixture lies within the limits of the Egyptian standard specification gradation (dense gradation 4 B). Table 3. represents the used mix gradation and corresponding specification Limits.

Asphalt concrete beams with 30 cm long (tested with 20 cm clear span), 5 cm width, and 6 cm height were prepared according to standard Marshall mix design method. Three asphalt contents are selected (4.5%, 5.0 %, and 5.5% A.C.) based on the value of optimum asphalt content calculated from Marshall test that equal 5.0 % . A steel mold was manufactured with inside dimensions of 30 * 5 * 8 cm. One piece of steel was prepared to simulate the initial crack depth of the specimen with initial cracks in field (Fig. 1).

Table 2: Properties of HaTelit c Product

Product	Unit	Spec. C 40/17
Raw Material		Polyester geogrid
Thickness	mm	2.0
Fabric Weight	gm/m^2	250
Mesh Size	mm	40 x 40
Open Area	%	min. 75
Ultimate Strength long./trans.	KN/m	50/50
Elongation at Break long./trans.	%	12/14
Heat Resistance	Up to 210 °C	

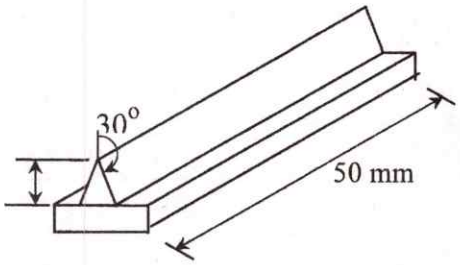

Fig.1: Steel Piece for Simulating initial Crack

Table 3:Aggregtae Gradation of Asphalt Concrete Mixture

Sieve size	% Passing	Spec. Limits
½	100	80-100
3/8	75	70-90
# 4	60	50-70
# 8	45	30-50
# 16	35	26-40
# 200	10	4-10

For each specimen, aggregate and binder were heated and mixed at 150 °C for 2 hours. A predetermined weight of hot mixture was placed in a prismatic steel mold in two layers. Each layer was tamped with a tamping rod. The mold was connected to a hydraulic press, and a flat steel plate 2 cm in thickness was placed on the top of the mixture. Static load was developed to compress the specimen to a desired height. This procedure produced a consistent specimen with the desired dimension and density. The specimens were compacted in two layers varying in thickness according to the cases shown in Table 4.

Table 4. Various Thickness of Layers with each Case

Case	Symbol	Description	First layer mm	Second layer mm
1	C.B.	Beam without reinforcement	30	30
2	W.G. ½	Beam with Alyaf PU 14 nonwoven geotextile at ½ depth	30	30
3	W.G. 1/3	Beam with Alyaf PU 14 nonwoven geotextile at the last third of depth	20	40
4	B.G. ½	Beam with HaTelit c geogrid at ½ depth	30	30
5	B.G. 1/3	Beam with HaTelit c geogrid at the last third of depth	20	40

3.3. Testing of Specimen

3.3.1.Testing of Beams without Initial Crack:

Three-point bending test was applied on the compacted asphalt concrete beams by using Computerized Universal Testing Machine. Firstly, the specimens were soaked in the water bath at a temperature of 20 °C for 45 minutes, then the test was performed with a constant rate of loading equal 3.0 mm/min. The load-deflection curve was obtained from the three-point bending test for each beam specimen.

Figure 2 shows the specimen on Computerized Universal Testing Machine during the test.

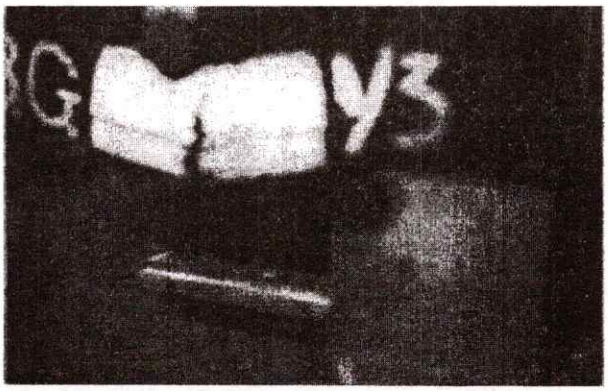

Fig.2 : The Specimen during the Test (at Failure)

3.3.2.Testing of Beams with Initial Crack

Testing of beams with initial crack is as previous test for beam without initial crack, but with an additional part for measuring the crack depth during the test interval. The crack depth was determined visually by observing the white painted part of the specimen every 30 second. Preliminary testing has been performed on a number of specimens to get the practice and experience to the adjustment of the beams and reading more one result at the same time.

4. ANALYSIS OF THE RESULTS

Analysis of the experimental results was performed on the direct measurements obtained from the test such as maximum stress and total absorbed energy. Moreover, two methods were used for evaluating the results of three-point bending test.

1)- The first method based on fracture mechanics approach. There are two fracture analysis approaches; the stress intensity approach and the energy criterion. The parameters that describe the stress intensity approach in case of linear – elastic condition are the fracture toughness K_{IC} and the fracture energy G_{IC} as indicated in Eq. (1, 2) [12].

$$K_{IC} = \frac{P\,S}{b\,d^{3/2}} \left[\frac{3\left(\frac{a}{d}\right)^{1/2}\left[1.99 - \frac{a}{d}\left(1-\frac{a}{d}\right)\left(2.15 - 3.93\left(\frac{a}{d}\right) + 2.7\left(\frac{a}{d}\right)^2\right)\right]}{2\left(1+2\frac{a}{d}\right)\left(1-\frac{a}{d}\right)^{3/2}} \right] \quad (1)$$

Where:
K_{IC} = Fracture toughness under plane- strain conditions, $N/m^{3/2}$.
P = Applied failure load, N.
S = Load span, m.
b = Specimen width, m.
d =Specimen height, m.
a = Notch depth, m.

It should be stated that, a large value of (k_{IC}) indicate that the material has higher resistance to crack propagation.

$$G_{IC} = \frac{K_{IC}^{\ 2}(1-V^2)}{E} = 0.84\frac{K_{IC}^{\ 2}}{E} \quad (2)$$

Where:
G_{IC} = Fracture energy or critical elastic energy release rate, J/m^2.
E =Young's modulus (obtained from the three-point bending test), N/m^2
v = Poisson's ratio (estimated to be 0.4)

The parameter that expresses the energy criterion in case of plasto – elastic condition is J-Integral, see Eq. (3).

$$J = \frac{2\,E}{d\,h_W} \quad (3)$$

Where:
J = The J-Integral parameter (J/m^2),
A=Area under the load versus load-line displacement,
d= Specimen thickness (depth).
h_w=Length of remaining unbroken ligament

2)- The second method is effective depth (german method) that based on the bending stress analysis. This method calculates the effective depth **hw** that sustains the load at failure hence the length of crack at failure **Z** can be obtained as shown from Eq. (4) to Eq. (12). This method assumes that the Load-Deflection Curve can be expressed by the following equation [13];

$$P = A_O \cdot W^{A_1} \cdot e^{A_2 \cdot W} \quad (4)$$

Where:
P = load, N
W = deflection, mm
Ao, A1, A2 are parameters

To determine these parameters (Ao, A1, and A2), logarithm of equation should be taken at every three points specially the point of changing slope such as A, B, and C, refer to Fig. 3.

Behavior of Cracks in Bending Test:

For a beam lied on two supports with a concentrated load in the middle, the stress, strain, and displacement (deflection) could be easily determined. The bending moment line can be determined from the following formula;

$$f(x) = \frac{M}{3\cdot E\cdot I}\bullet\left(\frac{3\cdot L\cdot X}{4} - \frac{X^3}{L}\right) \quad (5)$$

Behavior of Cracks in Bending Test:

For a beam lied on two supports with a concentrated load in the middle, the stress, strain, and displacement (deflection) could be easily determined. The bending moment line can be determined from the following formula;

Case of no–Cracks:

Deflection (w) increases as (x) increases and reaches the maximum value at a distance of x = L/2 from the support. So deflection can be calculated as follow;

$$f(x=L/2) = W = \frac{P\cdot L^3}{4\cdot b\cdot h_o^3 E} \quad (6)$$

Where ho is the thickness of the specimen in case of no–crack. From Eq. 6, the elastic modulus can be calculated from the following equation;

$$E = \frac{L^3}{4\cdot b\cdot h_o^3}\bullet\frac{P}{W} \quad (7)$$

This equation is more suitable for elastic materials, where the relation between the load and deflection is proportional. Because the asphalt has a viscous and plastic part beside the elastic part, the term P/W in Eq. 7 changes to dP/dW as indicated in Eq. 8.

$$E_{bz} = \frac{L^3}{4\cdot b\cdot h_o^3}\bullet A_o \bullet \begin{pmatrix} A_1\cdot W^{A_1-1}\cdot e^{A_2\cdot W} + \\ A_2\cdot W^{A_1}\cdot e^{A_2\cdot W} \end{pmatrix} \quad (8)$$

Bending stress can be obtained as follow;

$$\sigma_{bz} = \frac{3 \cdot L}{2 \cdot b \cdot h_o^2} \cdot A_o \cdot W^{A_1} \cdot e^{A_2 \cdot W} \qquad (9)$$

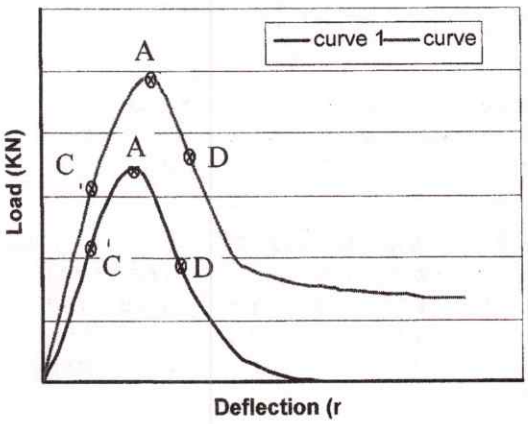

Fig. 3. Load – Deflection Curve for Control and Reinforcement Beams

Case of Cracks:

The cracks start to initiate from the tension area of the specimen at maximum load, point A of load – deflection curve.

Therefor the bending stress that calculated from Eq. 9 becomes fracture stress. The corresponding fracture strain ε_{bzA} is calculated from Eq. 10 as follow;

$$\varepsilon_{bzA} = \frac{6 \cdot h_o}{L^2} \cdot W_A \qquad (10)$$

During the formation of cracks, the cross section area of the specimen decreases. That is, the effective depth becomes smaller. This depth could be calculated in deflection rang W > WA from Eq. 11 as follow;

Effective depth hw

$$hw = \sqrt{\frac{3 \cdot L}{2 \cdot b \cdot \sigma_{bzA}} \cdot A_o \cdot W^{A_1} \cdot e^{A_2 \cdot W}} \quad \text{in mm} \qquad (11)$$

Crack depth Z is the deference between ho and *hw*

$$Z = ho - hw \quad \text{in mm} \qquad (12)$$

The percent of crack depth Zr % is as follow:

$$Zr = \frac{h_O - h_W}{h_O} \bullet 100 \qquad (13)$$

4.1. Analysis of Results for Beams Without Initial Crack:

The values of various parameters for beam specimens without initial crack are shown in Table 5.

4.1.1. Effect of Reinforcement on Max. Stress

Figure 4 shows the effect of reinforcement type and its position along the beam depth on max stress. It should be noted that the stresses in the case of reinforced beams are higher than that of unreinforced ones. Moreover the stresses achieved using **HaTelit c** reinforced geogrid are higher than that achieved by **Alyaf PU 14** geotextile at all asphalt contents. Also, using the reinforcement in the lower third of the beam depth gave higher stresses than of those in the middle depth for all asphalt contents and reinforcement types.

Moreover, it is observed from the curve that by using **HaTelit c** with 5.5 % A.C. at the lower third of the beam depth, case (5), the max. stress increases by 200 %, while at 5.5 % A.C. the max. stress elevates by 160 % for case (4). For **Alyaf PU 14**, it is noted that at 5.0 % A.C. the max stress increased by 90 % and 67 % for case (2) and (3) respectively.

Table 5. Values of Various Parameters for Beam without Initial Crack

A.C. %	Case	σ_a (N/mm^2)	Energy (N.m)	KIC (N/m$^{1.5}$)	GIC (J/m^2)	J-integral (J/m^2)	Z_r %
4.5 %	C.B. ½	2.52	11	49964	8	9477	36.8
	W.G. ½	3.25	39	64580	9	24428	17.4
	W.G. 1/3	3.75	41	74461	18	34323	16.0
	B.G. ½	4.00	57	79461	16	33929	14.9
	B.G. 1/3	6.34	84	125789	19	47704	11.5
5.0 %	C.B. ½	2.46	9	48825	7	7057	21.4
	W.G. ½	4.10	37	81481	16	22641	16.4
	W.G. 1/3	4.68	56	92895	18	35426	14.8
	B.G. ½	5.15	62	102165	19	39546	15.5
	B.G. 1/3	5.64	77	111923	27	47794	13.1
5.5 %	C.B. ½	3.04	12	60251	8	8638	22.3
	W.G. ½	3.11	26	61779	9	18450	19.2
	W.G. 1/3	5.39	31	107057	24	19531	17.0
	B.G. ½	7.85	81	155867	32	48893	13.7
	B.G. 1/3	8.98	108	178269	30	62547	10.1

It can be investigated that case (5) gave the best results of maximum stresses. **HaTelit c** indicated higher values of maximum stresses than that achieved by **Alyaf PU 14** because the modulus of elasticity in **HaTelit c** is higher than that in **Alyaf PU 14**. The main conclusion of these curves indicates that by involving the reinforcement through the beam depth, the resistance of beam to failure increases. This is because the reinforcement can absorb a significant proportion of the horizontal tensile stresses and ensures a uniform distribution of stress over a large area. So this function results in reducing the tensile stress peaks and the associated risks of overloading.

4.1.2. Effect of Reinforcement on Total Absorbed Energy

Figure 5 presents the effect of reinforcement type and its position along the beam depth on total absorbed energy for all asphalt contents. The total absorbed energy equals the area under the load-deflection curve. It should be noted from the Figure that the energy of the reinforced samples is greater than that of the unreinforced ones. Also, **HaTelit c**, gave higher values of energy than obtained by **Alyaf PU 14**, for all asphalt contents. In addition, the Figure shows that employing the reinforcement at the lower third of the beam depth exhibits higher values of energy than that achieved by the reinforcement at the middle for all asphalt contents too.

Also, it is clearly from the Figure that the lowest increase in the energy values occurred in case (2) at 5.5 % A.C. and equal 110 %, while the highest access that equal 740 % happened in case (5) at 5.5 % A.C. Also for **Alyaf PU 14**, the optimum asphalt content is 5.0 %, while 5.5 % A.C. is the optimum for **HaTelit c** reinforced geogrid.

4.1.3. Effect of Reinforcement on the Fracture Toughness K_{IC}

Figure 6 displays the effect of reinforcement type and its position along the beam depth on the fracture toughness K_{IC} for all asphalt contents. The Figure shows that the reinforced samples exhibit greater values of K_{IC} than the unreinforced ones.

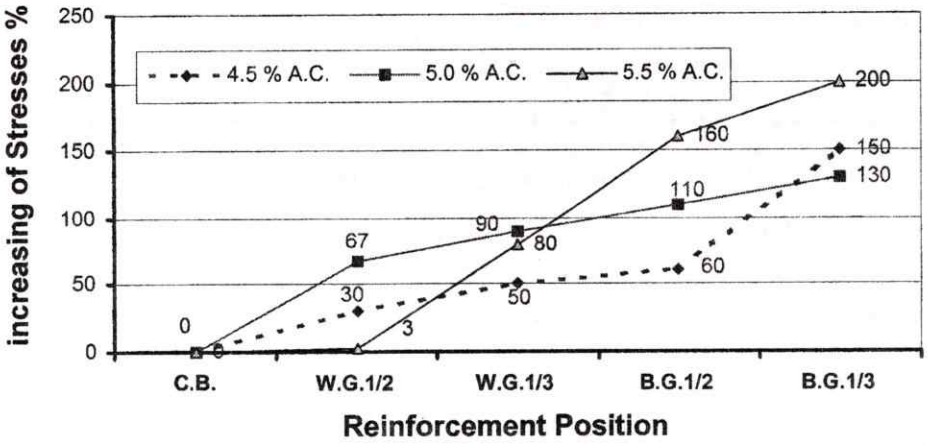

Fig. 4. Effect of the reinforcement Type and its Position in the Beam Depth on max Stress

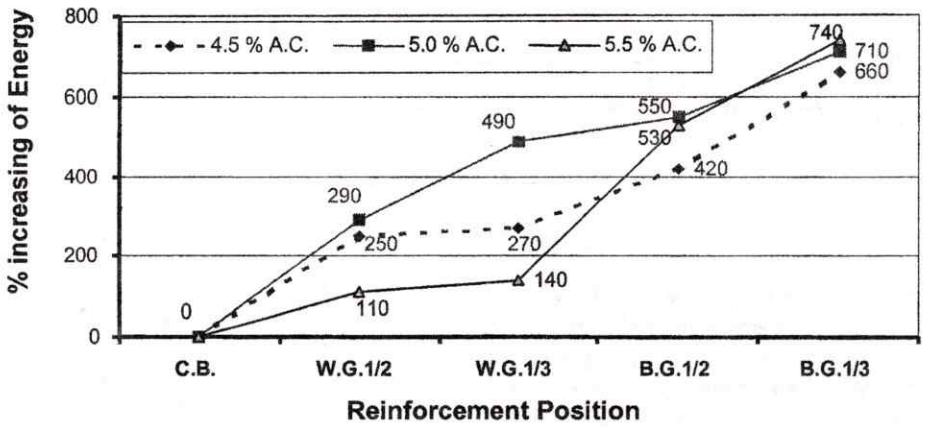

Fig. 5. Effect of the reinforcement Type and its Position in the Beam Depth on Total Absorbed Energy

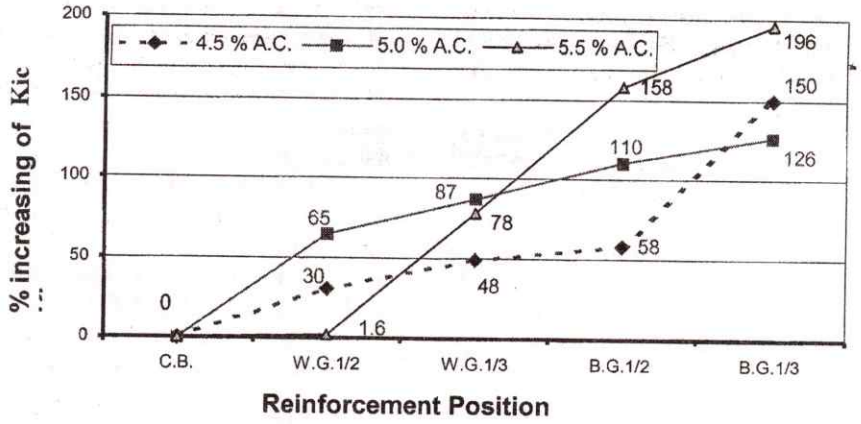

Fig. 6. Effect of the reinforcement Type and its Position in the Beam Depth on Fracture Taughness Kic

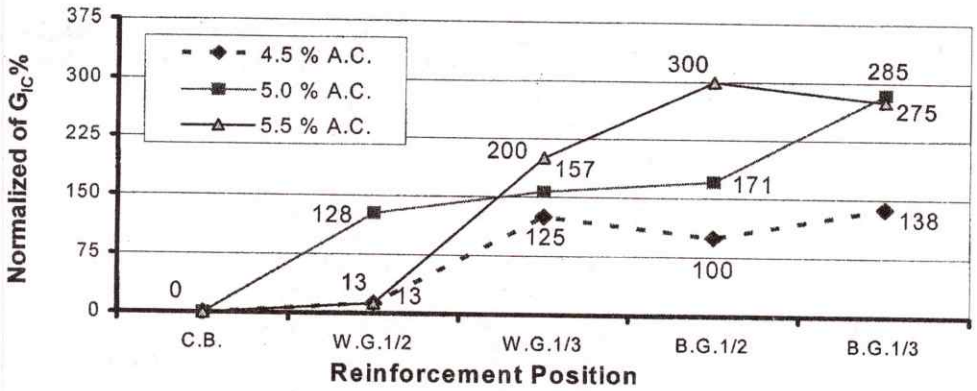

Fig.7. Effect of the reinforcement Type and its Position along the Beam Depth on Fracture Energy GIC

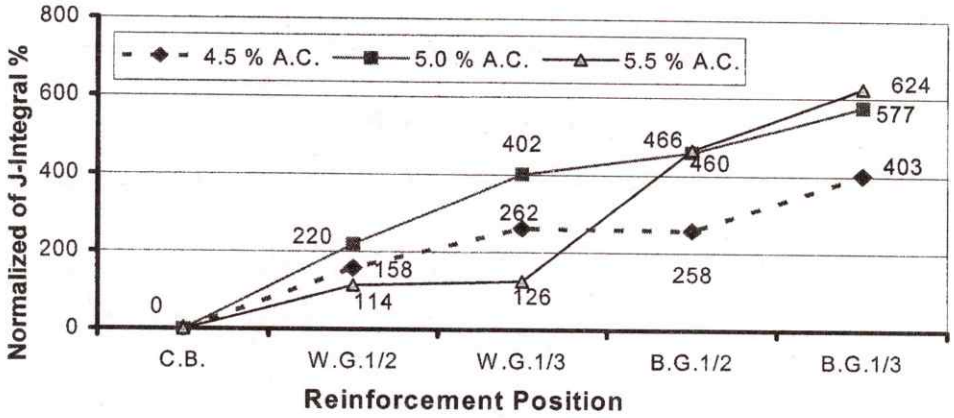

Fig.8. Effect of the reinforcement Type and its Position along the Beam Depth on J-Integral

This indicates that the material has a high resistance to failure and crack propagation in case of reinforced beams. Also, involving the reinforcement generally in the lower third of the beam depth gave higher values of K_{IC} than obtained from the usage of reinforcement in the middle for all asphalt contents too. Moreover, it can be observed that **HaTelit c** achieved values of fracture toughness more than that achieved by **Alyaf PU 14**.

It is clearly observed that the lowest access in K_{IC} values occurred in case (2) at 5.5 % A.C. and equal 1.6 %, while the highest increment in K_{IC} value that equal 196% happened in case (5) at 5.5% A.C. For **Alyaf PU 14**, the optimum asphalt content is 5.0 %,

while 5.5 % A.C. is the optimum for **HaTelit c**. Because of the fracture toughness depends on the maximum value of load and samples shape, the curves of K_{IC} resembles so much the curves of stresses.

4.1.4. Effect of Reinforcement on Critical Elastic Energy Release Rate G_{IC}

Firstly it is known that, the critical elastic energy G_{IC} is a quotient of two coefficients (fracture toughness K_{IC}) on (modulus of elasticity E). These moduli are considered, in origin, as an evidence for the strength of the material.

The effect of the reinforcement type and its position through the beam depth on the critical elastic energy release rate G_{IC} is represented in Figure 7 for all asphalt contents. The Figure shows that the reinforcement cases improve results of G_{IC} more than the unreinforcement cases.Also involving the reinforcement in the lower third of beam depth gave values of G_{IC} higher than that of employing the reinforcement in the middle at all asphalt contents except at 5.5 % A.C. for **HaTelit c** reinforced geogrid. The highest value was obtained in case (4) at 5.5 % A.C., while the lowest value occurred in case (2) at both 4.5 and 5.5 % A.C.

It is clear from the Figure that the largest access in G_{IC} value occurred in case (4) at 5.5 % A.C. and equal 300 %, while the lowest increase was 13 % and occurred in case (2) at both 4.5 and 5.5 % A.C. It was concluded from these curves that usage of the reinforcement results in an improvement in the elastic energy release rate G_{IC}.

4.1.5. Effect of Reinforcement on Elasto-Plastic Energy Release Rate J-Integral

The J-integral parameter has been developed to define the fracture conditions in material considering both elastic and plastic deformations. It has been developed as a result of the situations in which the crack tip was preceded by the development of a significant plastic zone.

Figure 8 produces the effect of reinforcement type and its position along the beam depth on elasto–plastic energy release rate J-integral for all asphalt contents. It is shown from the Figure that the reinforced samples achieved values of J-integral greater than the unreinforced ones for all asphalt contents. Moreover the usage of reinforcement generally in the lower third of the beam depth gave higher values of J-integral than that obtained from the usage of reinforcement in the middle. Also it can be observed that **HaTelit c** exhibits values of J-integral more than that achieved by **Alyaf PU 14.**

Also, it is observed that the lowest access in J-integral values occurred in case (2) at 5.5 % A.C. and equal 114 %, while the highest improvement equal 624 % and occurred in case (5) at 5.5 % A.C. Also for **Alyaf PU 14**, the optimum asphalt content is 5.0 %, while 5.5 % A.C. is the optimum for **HaTelit c.**

4.1.6. Effect of Reinforcement on the Crack Depth Ratio Zr

Effect of reinforcement type and its position along the beam depth on the crack depth ratio, **Zr**, was determined at 4.5, 5.0, and 5.5 % A.C. Figure 9 shows, as example, this relationship at 5.0% A.C. It should be stated that the lowest **Zr** value, the more resistance to crack propagation. It can be concluded that the reinforced specimens gave values of **Zr** smaller than that obtained from unreinforced ones.

Moreover, the usage of reinforcement in the lower third of the beam depth exhibited results better than that obtained from the usage of reinforcement in the middle. Also **HaTelit c** achieved results better than the first type **Alyaf PU 14**.

Also, it can be concluded that the involving of **HaTelit c** in the lower third of the beam gave the best results of resistance to crack propagation. Also it is important to point out that these results coincide with the previous results obtained from cases of stresses, energy, K_{IC}, and J-integral.

4.2. Analysis of Results for Beams With Initial Crack

The values of various parameters for beam specimens with initial crack are shown in Table 6. It must be observed that all results were obtained at 5.0 % A.C.

Table 6 : Values of Various Parameters for Beam with Initial Crack

A.C. %	Case	σ_a (N/m m^2)	Energy (N.m)	K_{IC} (N/m$^{1.5}$)	G_{IC} (J/m^2)	J-integral (J/m^2)	Z_r %
5.0%	C.B. ½	2.3	9	2.9E+5	207	5585	21.9
	W.G. ½	3.9	33	5.0E+5	577	22547	18.7
	W.G. 1/3	4.2	42	5.3E+5	591	24607	15.3
	B.G. ½	4.8	50	6.2E+5	709	28826	17.2
	B.G. 1/3	5.5	58	7.0E+5	1075	35221	14.3

4.2.1. Effect of Reinforcement on Max. Stress, absorbed energy, fracture toughness (Kic), fracture energy (Gic) and J-integral

Figure 10 produces the effect of reinforcement type and its position along the beam depth on normalized effect of maximum stresses, absorbed energy, fracture toughness (Kic), fracture energy (Gic) and J-integral for beams with initial crack at 5.0% asphalt content. It should be observed that these last parameters were increased by using geotextile as a

reinforcement. Also max stress, total absorbed energy, fracture toughness (Kic), fracture energy (Gic) and J-integral obtained by **HaTelit c** reinforced geogrid are more than that achieved by **Alyaf PU 14** reinforced nonwoven geotextile. In addition, usage of the reinforcement in the lower third of beam depth exhibited higher values of the all mentioned parameters than that of others in the middle depth for all types of reinforcement.

The important conclusion of these curves not differs from the case of beam without initial crack. This indicates that by involving the reinforcement in the beam depth, the stresses increase. That is the load spreading is improved resulting in more resistance to failure and crack propagation.

This means that the required energy for crack growth to reach the critical state increased by 5.31 times. This improvement in J – Integral values makes the layers containing the reinforcement to service well for a long time resulting in prolonging the lifetime of the road. Hence the maintenance cost will decreases. These results coincide with the results of stresses, energy, and fracture toughness in that case (5) is the optimum case to getting best results in improvement the resistance of the asphalt layers.

4.2.2. Effect of Reinforcement on the Crack Depth Ratio Zr

The effect of reinforcement type and its position along the beam depth on the crack depth ratio, Zr, at A.C.= 5.0 % is illustrated in Figure 11. As stated before the lowest Zr value, the more resistance to crack propagation. This means that the crack grows in a slow manner if Zr decreases. From the Figure it can be concluded that the reinforced specimens achieved values of Zr lower than that obtained from unreinforced ones. Moreover, the involving of reinforcement in the lower third of the beam depth exhibited results better than that obtained from the usage of reinforcement in the middle. HaTelit c reinforced geogrid achieved results better than the first type Alyaf PU 14 reinforced nonwoven geotextile.

4.2.3.Crack Depth Curve of Beams with Initial Crack

Figure 12 indicates the time-crack depth curve for beams with initial crack for all cases of reinforcement. It is observed that the cracks grow in the reinforced cases with a rate lower than that of unreinforced one. This indicates that the reinforcement provides more tensile strength to the asphalt layers that making them arrest or relevant the propagation of the cracks through the new overlay. Thus the reflective cracking can be retarded leading to prolong the lifetime of the pavement.

Figure 12 shows that case (5), B.G. 1/3, achieved the lowest curve that is, the crack grows slowly more than the other cases. Thereby this result complies with the conclusions of **Zr** discussion. So the reinforcement section subjects to a lower distresses than the unreinforcement ones.

It can be stated that the rate of crack growth may give an idea of the thickness of the overlay that needs to be provided for different design life periods. It was observed during the test that the presence of aggregate particles along the crack path dictated a longer travel distance of the crack and consequently decreased the rate of crack growth. Also the rupture in the unreinforced test specimen occurred in a single wide crack form, while the reinforced test specimen, whether with or without initial crack, exhibited a finely distributed cracks in the bottom of tested beam because of the load – distribution effect of the reinforcement.

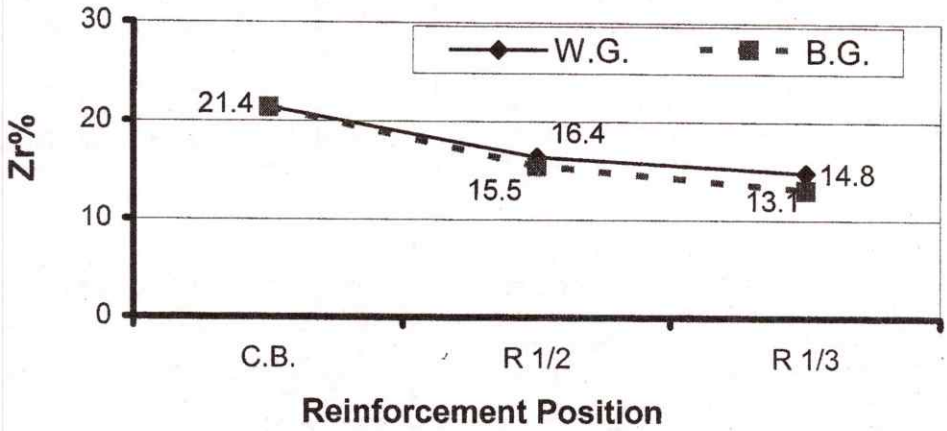

Fig.9. Effect of Reinforcement Type and its Position along the Beam Depth on Crack Depth Ratio Zr at A.C.= 5.0 %

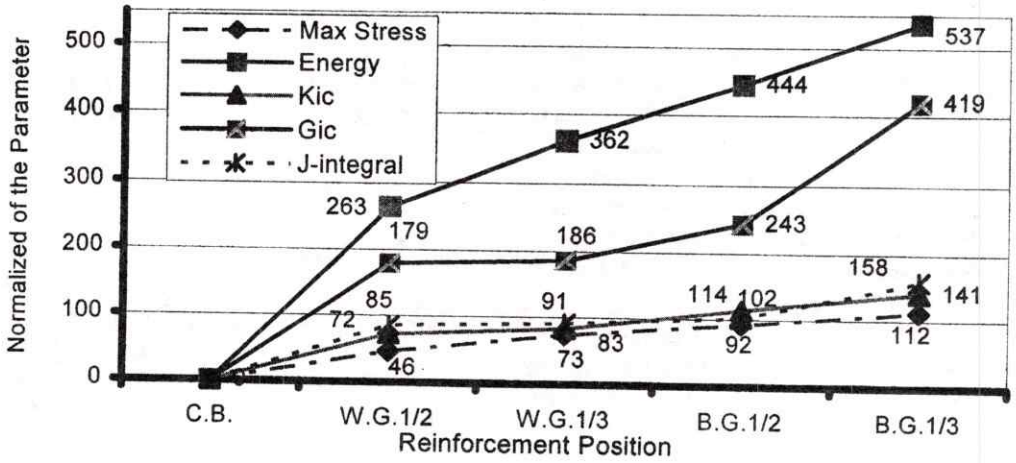

Fig. 10. Effect of the Reinforcement Type and its Position along the Beam Depth on Max Stress, Energy, Kic, Gic and J-integral

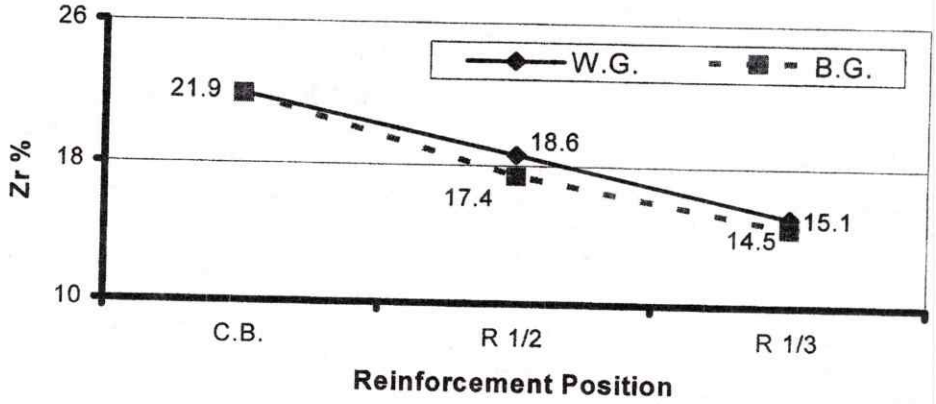

Fig. 11. Effect of Reinforcement Type and its Position in the Beam Depth on Crack Depth Ratio Zr at A.C.= 5.0 %

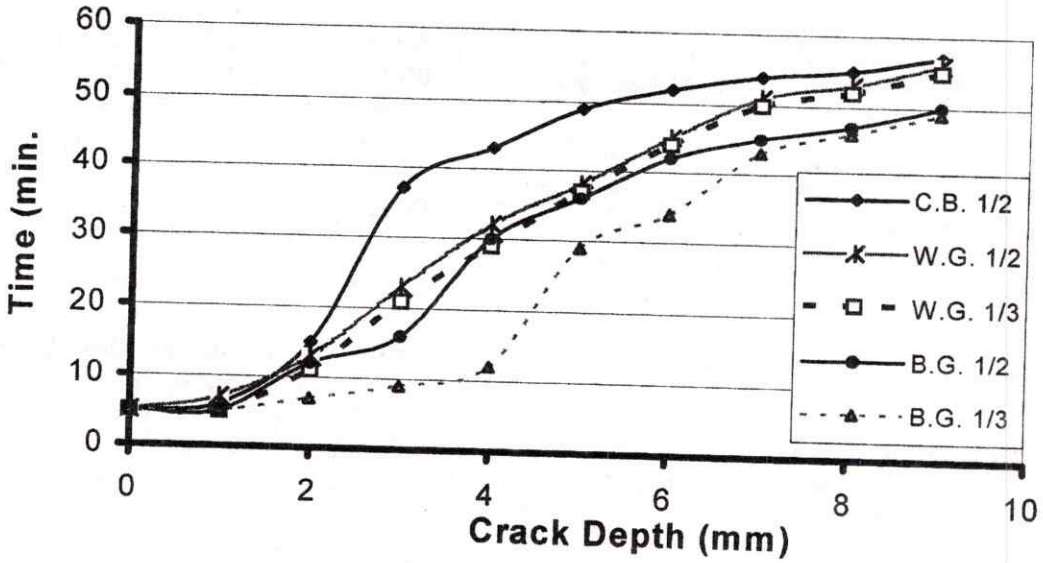

Fig. 12 Time–Crack Depth Curve for all Cases of Reinforcement

5. CONCLUSIONS

1- The placement of reinforcement between the cracked or uncracked layers and the new overlay can improve the load – carrying capacity of pavement structure via absorbing a significant proportion of the horizontal tensile stresses in the asphalt layer and ensures a uniform distribution of stress over a large area. So this function results in reducing the tensile stress peaks and the associated risks of overloading. In addition to increase the tensile strength of the asphalt layer.

2- Using the reinforcement at the lower third of the overlay depth showed results in resistance to the crack propagation better than involving it in the middle of the overlay depth.

3- It is observed during the test that the separation between the tested asphalt layers and reinforcement did not occurred and this emphasizes that the good sticking between the reinforcement that lie between the old and new layers is required. Also the rupture in the unreinforced test specimens occurred in the form of a single wide crack, while a finely distributed cracks appeared in the bottom of the reinforced test specimens.

4- **HaTelit c** reinforced geogrid achieved results in crack propagation resistance and strengthening the asphalt layers higher than **Alyaf PU 14** reinforced nonwoven geotextile at all asphalt contents and for all positioning of the reinforcement.

5- The optimum asphalt content for **HaTelit c** geogrid is 5.5 %, while 5.0 % A.C. is the optimum for **Alyaf PU 14** nonwoven geotextile.

6- Involving **HaTelit c** geogrid at the lower third of the overlay depth placed over uncracked layer with 5.5 % A.C.

-Increasing the strength of the pavement structure by increasing the value of max stress with a percent of 200 %.

-Increasing service life of the pavement by increasing the total absorbed energy with a percent of 740 %.

-Increasing fracture toughness K_{IC}, fracture energy G_{IC}, and J–Integral by 196, 275, and 624 % respectively.

-Reducing the crack depth ratio, Zr, from 22.3 % to 10.1 %.

7-Involving **Alyaf PU 14** nonwoven geotextile at the lower third of the overlay depth placed over uncracked layer with 5.0 % A.C.

-Increasing the strength of the pavement structure by increasing the value of max stress with a percent of 90 %.

-Increasing service life of the pavement by increasing the total absorbed energy with a percent of 490 %.

-Increasing fracture toughness K_{IC}, fracture energy G_{IC}, and J–Integral by 87, 157, and 402 % respectively.

-Reducing the crack depth ratio, Zr, from 21.4 % to 14.8 %.

8-Involving **HaTelit c** geogrid at the lower third of the overlay depth placed over cracked layer, simulated with initial crack, at 5.0 % A.C. increased max stress, energy, K_{IC}, G_{IC}, and J–Integral by 139, 537, 141, 419, and 158 % respectively. In addition, it reduced Zr from 28 % to 14 %.

9-Involving **Alyaf PU 14** nonwoven geotextile at the lower third of the overlay depth placed over cracked layer with 5.0 % A.C. increased max stress, energy, K_{IC}, G_{IC}, and J–Integral by 83, 362, 83, 186, and 91 % respectively. Also Zr reduced from 28 % to 15 %.

10-**HaTelit c** geogrid and **Alyaf PU 14** nonwoven geotextile have moduli of elasticity equal 6640 N/mm^2 and 920 N/mm^2 respectively. And this fact interpolates the better performance of **HaTelit c** geogrid than **Alyaf PU 14** nonwoven geotextile.

11-It is observed during the test that the presence of aggregate particles along the crack path dictated a longer travel distance and thus higher fracture toughness and lower crack growth were achieved.

REFERENCES

[1] German, F. P. and Lytton, (1999). "Methodology for Predicting The Reflection Cracking Life of Asphalt Concrete Overlays", Rep. FHWA/TX99/09+207-5, Federal Highway Administration, College Station, Texas.

[2] Samanos, J. and Tessonneau, H., (March 1993). " New System for Preventing Reflective Cracking: Membrane Using Reinforcement on Site (Murmos) ", proceeding of 2nd International RILEM conference, Liege university, Belgium.

[3] J. M. Rigo, (March 1993). "General Introduction, Main Conclusion of The 1989 Conference on Reflective Cracking in Pavement, and Future Prospect", proceeding of 2nd International RILEM conference, Liege university, Belgium.

[4] Harold L. Von Quintus, Harvey J. Treybig, and Frank M. Cullough, (1979). " Reflection Cracking Analysis For Asphalt Concrete Overlays ", The Association of Asphalt Paving Technologists (AAPT), pp. 477-506.

[5] B.J. Dempsey, (2002). " Development and Performance of Interlayer Stress Absorbing Composite (ISAC) In Ac Overlays ", Prepared for 81 st Transportation Research Board Annual Meeting.

[6] Ponniah E. Joseph, (1987). "Low Temperature Reflection Cracking Through Asphalt Overlays ", A Thesis Presented To The University of Waterloo For The Degree of Doctor of Philosophy.

[7] Barzin Mobasher, Michel S. Mamlouk, and How-Ming Lin, (1997). "Evaluation of Crack Propagation Properties of Asphalt Mixtures", Journal of Transportation Engineering, pp. 405-413.

[8] G. S. Cleveland, R. L. Lytton, and J. W. Button, (2003). " Reinforcing Benefits of Geosynthetic Materials in Asphalt Concrete Overlays using PseudoStrain Damage Theory ", Prepared for 82 nd Transportation Research Board Annual Meeting.

[9] A khtar Hussein A. Tayebali, Geoffrey M. Rowe and Jo rge B . S ousa, (1992). " Fatigue Response of Asphalt-Aggregate Mixtures", The Association of Asphalt Paving Technologists (AAPT), pp. 333-360.

[10] Mc Asphalt Industries Limited Scarborough, Ontario, (February 2, 1995). "Superpave- The System ", Carleton University, Civil Engineering Department.

[11]Jacobs, M. M. J., P. C. Hopman, a nd A . A . A . Molenaar (1996). "Application of Fracture Mechanics Principles to Analyze Cracking in Asphalt Concrete". I n *P roc. Annual Meeting of the Association of Asphalt Paving Technologists*, Vol. 65, Baltimore, MD, pp. 1-39.

[12] Todd R. Hoare and Simon A. M. Hesp, (January 2000). " Low- Temperature Fracture Testing o f Asphalt Binders: Regular and Modified Systems", Transportation Research Board, 79 th Annual Meeting, 9-13, Paper No. 1234. International RILEM conference, Liege university, Belgium.

[13] Dr.-Ing. B. Gratz, (1985). " Einfluß der Kornmerkmale und der Hohlräume einer Deckschicht aus asphaltbeton auf deren Biegezug- und Risseverhalten" , Darmstadt, Bitumen 2/1985.